Precision measurement of the $3d\ ^2D_{3/2}$–state lifetime in a single trapped $^{40}Ca^+$

H. Shao,[1,2,3] Y. Huang,[1,2] H. Guan,[1,2,*] Y. Qian,[1,2,3] and K. Gao[1,2,†]

[1]*State Key Laboratory of Magnetic Resonance and Atomic and Molecular Physics, Wuhan Institute of Physics and Mathematics, Chinese Academy of Sciences, Wuhan 430071, China*

[2]*Key Laboratory of Atomic Frequency Standards, Wuhan Institute of Physics and Mathematics, Chinese Academy of Sciences, Wuhan 430071, China*

[3]*University of the Chinese Academy of Sciences, Beijing 100049, China*

(Received 3 July 2016; published 10 October 2016)

We present a high-precision measurement of the $3d\ ^2D_{3/2}$–state lifetime in a single trapped $^{40}Ca^+$. The measurement was performed using a high-efficiency quantum-state detection technique to monitor quantum jumps and a high-precision and highly synchronous measurement sequence for laser control. A feature in our measurement is the pumping rate of the 729-nm laser that was corrected in a real-time way. The $3d\ ^2D_{3/2}$–state lifetime was obtained through the measurement of the spontaneous decay rate after incoherent shelving of the ion to the $3d\ ^2D_{3/2}$ state with a wait time. Systematic errors, such as collisions with background gases, heating effects, impurity components, the shelving and pumping rates, and state detection, were carefully analyzed and estimated. We determined an improved value of the $3d\ ^2D_{3/2}$–state lifetime to be $\tau_{3/2} = 1.195(8)$ s. Furthermore, the $3d\ ^2D_{3/2} \rightarrow 4s\ ^2S_{1/2}$ quadrupole transition matrix element was measured to be $S_{ki} = 7.936(26)ea_0^2$, and the ratio between the lifetimes of $3d\ ^2D_{3/2}$ and $3d\ ^2D_{5/2}$ was determined to be 1.018(11). Our method can be universally applied to lifetime measurements of other single ions and atoms with a similar structure.

DOI: 10.1103/PhysRevA.94.042507

I. INTRODUCTION

A single $^{40}Ca^+$ ion confined in a miniature ring Paul trap is an ideal system for studying various domains of atomic physics, including the precision atomic spectrum [1], quantum information [2–5], astronomy-related aspects [6,7], transition strengths [8], and radiative lifetimes [9–11], owing to its isolation from the environment and long trap time, which provide a way to have stable interrogation times and small systematic errors. Among these applications, the $4s\ ^2S_{1/2} \leftrightarrow 3d\ ^2D_{3/2}$ quadrupole transition has been used to encode a bit of information for storing and processing quantum information [2–5] due to the long lifetime of the $3d\ ^2D_{3/2}$ state. Also, the $^{40}Ca^+$ quadrupole absorption lines can provide information on structure and physical characteristics of interstellar clouds [6,7]. Moreover, experimental data for the $3d\ ^2D_{3/2}$ lifetime is useful for a direct test of atomic wave functions [11–20]. However, a precision measurement of the $3d\ ^2D_{3/2}$ lifetime is limited by the character of atomic structure, unlike the $3d\ ^2D_{5/2}$ state, which can be realized effectively by a direct state detection. Here, we report a measurement method with a real-time nature, in which a repumping rate is introduced to precisely reflect the pumping rate, a key factor for determining the accuracy of the $3d\ ^2D_{3/2}$–state lifetime measurement. Our method has solved the problem of the ion's condition changing with wait time after spontaneous decay.

The radiative lifetimes of various states of $^{40}Ca^+$ have recently been measured by several groups. Hettrich *et al.* measured the lifetime of the $4p\ ^2P_{1/2}$ state using a method that compared measurements of dispersive and absorptive light-ion interactions [8]. Their measured lifetime, however, disagrees with the one by Jin and Church, who used a variant of the collinear laser-beam–ion-beam spectroscopy technique [21]. The lifetime of the metastable $3d\ ^2D_{5/2}$ state was measured directly by using the electron-shelving method [9,22] and by a high-efficiency quantum-state detection technique that involves no laser disturbance of the spontaneous decay [10,11]. These two direct measurement methods give rise to results that are in very good agreement. However, only a few measurements of the lifetime of the $3d\ ^2D_{3/2}$ state have been conducted. The first such measurement is due to Arbes *et al.* [23], who used a single ion. Their measured lifetime is 1.113(45) s. Later, laser cooling technology was applied to the ion cloud by Knoop *et al.* [24] and to a stored ion beam by Lidberg *et al.* [25], the resulting lifetimes being, respectively, 1.111(46) and 1.170(50) s. Recently, with the development of ion-trapping technology and laser spectroscopy methods, Barton *et al.* [9] obtained the improved value of the $3d\ ^2D_{3/2}$ lifetime, 1.20(1) s, by combining a measured lifetime of the $3d\ ^2D_{5/2}$ state [$\tau_{5/2} = 1.168(7)$s] with the theoretical lifetime ratio $\tau_{3/2}/\tau_{5/2} = 1.026(7)$. Kreuter *et al.* [11] performed a measurement on a single ion trapped in a linear Paul trap, using a method similar to that in [26]. Their result of 1.176(11) s is, however, in disagreement with the value of Barton *et al.* [9]. The current status of the determination of the $3d\ ^2D_{3/2}$ lifetime is summarized in Fig. 1.

Motivated by resolving experimentally the above-mentioned discrepancy between the two most recent measurements [9,11], here, we present an improved method for the $3d\ ^2D_{3/2}$–state lifetime measurement. The experiment was performed by an indirect technique based on high-efficiency quantum-state detection that was used to monitor quantum jumps and a high-precision and highly synchronous measurement sequence for laser control. We adopted a scheme with a real-time nature for correcting the 729-nm pumping rate, which increased the effective pumping rate to approximately 100%. This scheme can precisely reflect the ion's condition in real time. By measuring the unperturbed spontaneous decay

*guanhua@wipm.ac.cn
†klgao@wipm.ac.cn

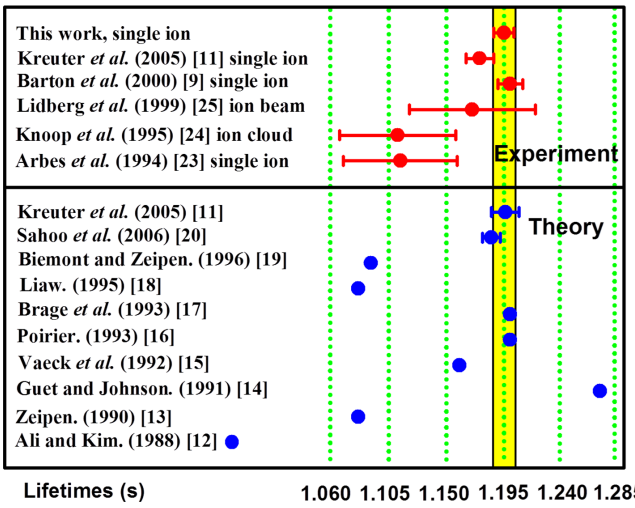

FIG. 1. Comparison of theoretical and experimental results for the lifetime of the $3d\ ^2D_{3/2}$ state, in seconds.

rate of the ion in the $3d\ ^2D_{3/2}$ state with wait time, an improved value of the lifetime was determined to be $\tau_{3/2} = 1.195(8)$ s, which agrees well with the result of Barton *et al.* [9]. More importantly, our measured lifetime is also in good agreement with the most recent theoretical result of 1.196(11) s by Kreuter *et al.* [11] and of 1.185(7) s by Sahoo *et al.* [20]. Our method can, in principle, be applied to other single-ion systems, such as Mg^+, Ba^+, and Sr^+, for lifetime measurements.

II. EXPERIMENTAL PROCEDURE

A single $^{40}Ca^+$ ion was confined in a miniature ring Paul trap similar to the one in [10]. The trap was composed of a ring, two endcap electrodes, and two compensation electrodes. Adjusting the voltage of the endcap and compensation electrodes can effectively control the ion's excess micromotion. An important advantage of this trap is its open structure, which is very suitable for the interaction between ions and lasers during cooling, pumping, and detection. Furthermore, in order to reduce the deexcitation caused by collisions between the ion and background gases and to ensure an ideal stable environment for the measurement, the ion trap was installed in an ultrahigh vacuum chamber with a background pressure $<1.0 \times 10^{-8}$ Pa. The ion was Doppler cooled primarily using the $4s\ ^2S_{1/2} \leftrightarrow 4p\ ^2P_{1/2}$ dipole transition with 397-nm wavelength for the short lifetime of the excited state [8]. A power of 10.2 μW and a beam waist of 40 μm were applied. Because of the decay branching from the $4p\ ^2P_{1/2}$ state to the $3d\ ^2D_{3/2}$ state [27], an 866-nm laser with a power of 450 μW and a waist of 80 μm was used to evacuate the ion from this state. To prepare the initial $3d\ ^2D_{3/2}$ state for spontaneous decay, the 397-nm laser was also used to incoherently shelve the ion to that state when the 866-nm light was absent. Here, we point out that the state $3d\ ^2D_{3/2}$ is different from the state $3d\ ^2D_{5/2}$ in the sense that the former can be connected to $4p\ ^2P_{1/2}$ by an electric-dipole-allowed transition. An attempt to detect the fluorescence by turning on the two lasers of 397 and 866 nm would destroy the state of the freely decaying ion. Thus one needs to leave the ion unperturbed in the $3d\ ^2D_{3/2}$ state for a while to determine whether a spontaneous decay occurs. In this work, we adopted an indirect method for the measurement of the $3d\ ^2D_{3/2}$ state. We allowed the ion to decay spontaneously without any perturbation for a specific wait time, and we then determined whether the ion was decayed to the ground state by applying a pumping laser to excite the ion to the $3d\ ^2D_{5/2}$ state. A typical narrow-linewidth ($\sim$1 Hz) Ti:sapphire laser (Coherent Inc., MBR110) of 729 nm was adopted [28], which was locked to a high-finesse Ultra-low-expansion (ULE) cavity according to the Pound-Drever-Hall scheme to pump the ion to the $3d\ ^2D_{5/2}$ state. The power of the laser was 9.8 μW, and the beam waist was 100 μm. The quenching of the ion from the $3d\ ^2D_{5/2}$ state was accomplished by applying an 854-nm laser with a power of 160 μW and a waist of 80 μm. In order to realize multiperiod continuous measurement, both the 397- and 866-nm lasers were frequency stabilized to the ultranarrow-linewidth 729-nm laser by a transfer cavity [29]. The signal detection relied on the 397-nm fluorescence generated by the spontaneous decay of the ion from the $4p\ ^2P_{1/2}$ state to the $4s\ ^2S_{1/2}$ state and was monitored by a photomultiplier tube (PMT; ET Enterprises, 9893Q/100B). The scattered background light was filtered by a narrow-band-pass filter and a pinhole with a diameter of 500 μm from the fluorescence signal. A photon counter (Stanford Research Systems, SR400) was used to record the amplified signal after the PMT. A computer recorded all experimental data and controlled the photon counter, all acousto-optic modulators (AOMs), and shutters simultaneously via a PIC-6733 DAQ card at the accuracy of the microsecond level.

A simplified sequence and relevant level diagrams describing the lifetime measurement of the $3d\ ^2D_{3/2}$ state are depicted in Fig. 2. This sequence consists of four major steps for a valid round of measurement. In the first step, the 397- and 866-nm lasers were employed for the cooling cycle, and the ion was laser cooled to the Lamb-Dicke regime. Meanwhile, the 854-nm quenching laser was applied to excite the ion from the $3d\ ^2D_{5/2}$ state to the $4p\ ^2P_{3/2}$ state, ensuring that the ion was laid in the ground state. Subsequently, a 3-ms 397-nm laser of 10.2 μW power excited the ion through the $4s\ ^2S_{1/2} \rightarrow 4p\ ^2P_{1/2}$ transition to induce an incoherent shelving to the $3d\ ^2D_{3/2}$ state. In the second step, all the lasers were switched off, followed by a wait period, during which the ion was decayed spontaneously with no lights disturbing the process. In the third step, to verify whether the ion was decayed from the $3d\ ^2D_{3/2}$ state to the ground state, a 3-ms 729-nm laser was applied. If the ion was decayed to the $4s\ ^2S_{1/2}$ state, it could be pumped to the $3d\ ^2D_{5/2}$ state, and the photon count decreased to the background level. To eliminate the magnetic field at the ion's position, we kept a stable pumping rate of the 729-nm laser; the Hanle effect was adopted, and the ten Zeeman spectrum lines were recorded with a full width of approximately 500 Hz. However, the ion could not be fully pumped by the 729-nm laser in every period because it was not possible to realize the state preparation, as the rate was only approximately 50% (red line in Fig. 3). In addition, after the wait time, the ion's condition could change due to pumping laser frequency shift and magnetic-field noise caused by the environment, resulting in a reduction of the stability of the pumping rate (blue line in Fig. 3). Therefore, in the last step, a pumping rate of 729 nm was accurately measured in real time.

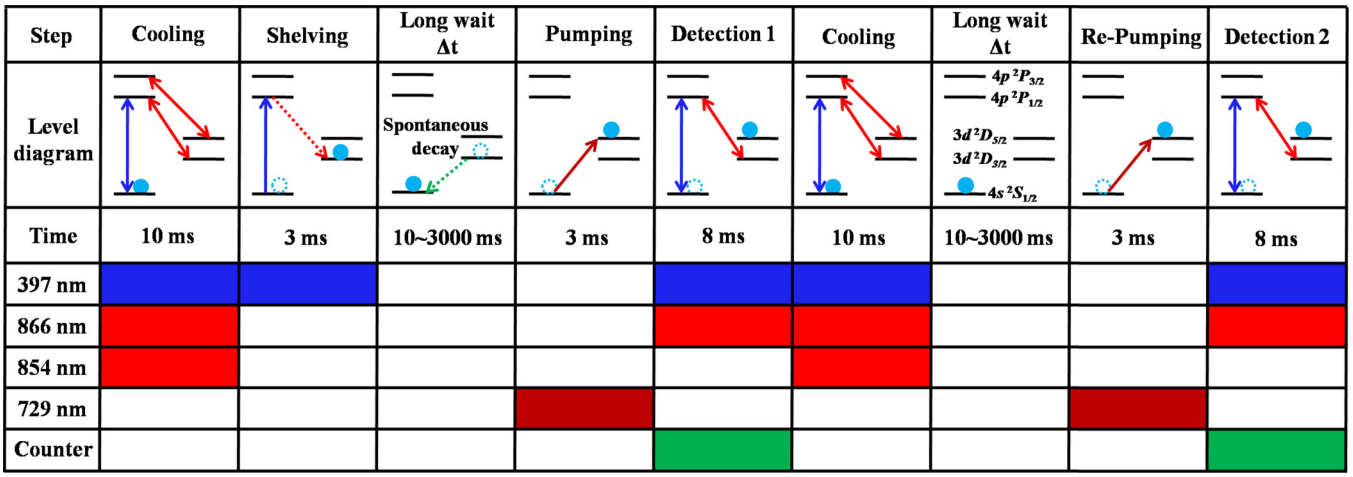

FIG. 2. The simplified sequence and partial energy-level diagrams of $^{40}Ca^+$ showing the spontaneous decay from the metastable $3d\ ^2D_{3/2}$ state to the $4s\ ^2S_{1/2}$ ground state for the lifetime measurement. The 397- and 866-nm lasers are for cooling, the 854-nm laser is for quenching, the 729-nm laser is for pumping, and the combined 397- and 866-nm lasers are for fluorescence detection.

III. RESULTS

We first eliminated in a real-time way the effect of environment and successfully corrected the 729-nm pumping rate. As a specific design for state detection described above, we should pump the $4s\ ^2S_{1/2}$–state ion to the $3d\ ^2D_{5/2}$ state after spontaneous decay. This process brought in an additional pumping rate of the 729-nm light to the measurement, which determined the final accuracy of the $3d\ ^2D_{3/2}$ lifetime. However, this rate could not be directly obtained in the lifetime measurement and should thus be measured separately. In order to determine precisely the pumping rate, we need to introduce the repumping rate. We found that if we did not have a wait time after the second cooling cycle, the repumping rate would remain stable (red line in Fig. 3); however, in reality, the ion's condition changed with wait time (blue line in Fig. 3), and thus, the pumping rate was no longer stable. Thus, we could not take the first rate to mirror the true pumping rate of 729 nm, and a real-time way was needed. Our method was to introduce a wait time Δt after the second cooling process using the 397- and 866-nm lasers while the 854-nm quenching laser was applied. For this method, we repeated a sequence, which excluded the 397-nm laser shelving to $3d\ ^2D_{3/2}$, several thousand times during every Δt varying from 10 to 3000 ms. Thus, the pumping rate could be reflected accurately by the repumping rate; the only difference was no decay process compared to the lifetime measurement. The pumping P_p and repumping P_{r-p} rates are, respectively, defined as the ratio of the number of quantum jumps counted in the first (N_1) and second (N_2) detection periods to the number measured in the total repeated period N (blue and pink lines in Fig. 3). In each Δt, the ratio was $P_{r-p}/P_p \approx 1$, which means that the effective pumping rate was approximately 100% (green line in Fig. 3). Here, we have demonstrated that the pumping rate of the 729-nm laser for different wait times Δt after the cooling period can reflect the condition of the ion in a real-time way.

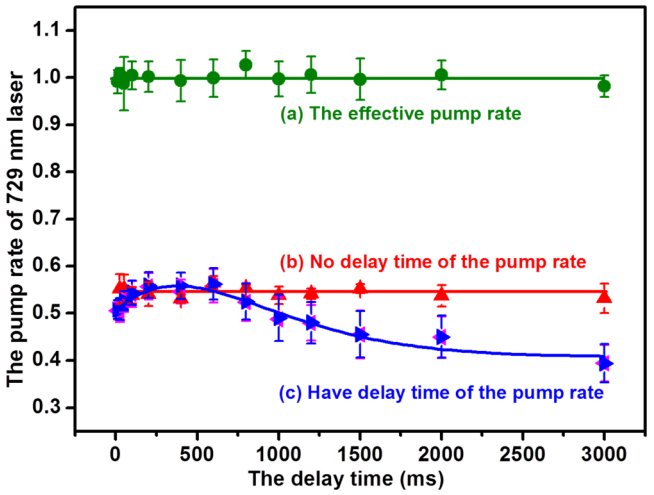

FIG. 3. The pumping rate of the 729-nm laser measured in a real-time way to reflect the condition of the ion for different Δt periods. The effective pumping rate is approximately 100%. Each data point was measured 3000 times.

When the ion is shelved to the $3d\ ^2D_{3/2}$ state, a spontaneous decay occurs. With the full measurement sequence performed, the detected decay rate $P_{\rm exp}$ is the ratio of the number of quantum jumps counted in the first detection period N_1 to that measured in the total repeated period N. However, considering that the pumping pulse excites the electron to the $3d\ ^2D_{5/2}$ state with the probability $P_{r-p} = N_2/N$, the final decay rate is $P = P_{\rm exp}/P_{r-p} = N_1/N_2$. Therefore, the decay probability P is defined as the ratio of the number of quantum jumps counted in the first detection period N_1 to the number counted in the second detection period N_2. The lifetime of the $3d\ ^2D_{3/2}$ state is then obtained from the exponential function $1 - P = \exp(-\Delta t/\tau_{3/2})$. The above four steps were repeated 25 000 times per Δt in our experiment, where Δt was set to vary from 10 to 3000 ms. The results are shown in Fig. 4.

IV. EVALUATION OF UNCERTAINTIES

The observed lifetime of the $3d\ ^2D_{3/2}$ state is affected by many factors, such as collision effects, ion heating, impure composition and coupling of lasers, and the pumping rate,

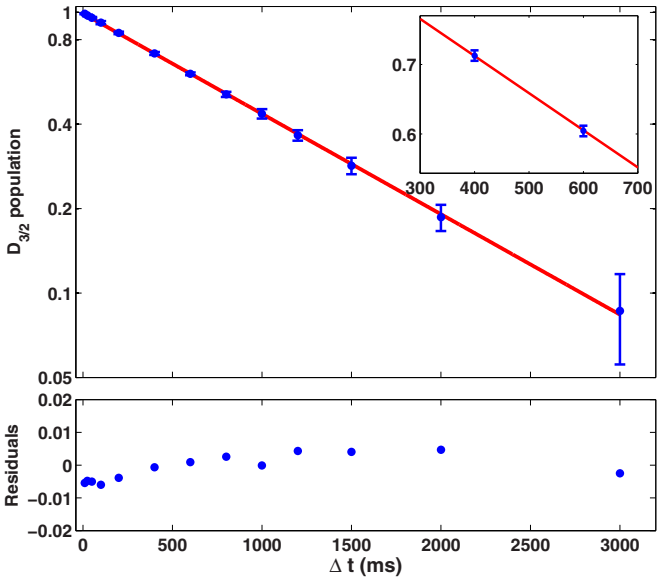

FIG. 4. The decay probability of the $3d\ ^2D_{3/2}$ state for delay time from 10 to 3000 ms. Each point represents 25 000 measurements per Δt. The solid red line denotes the linear regression, and a least-squares fitting yields the lifetime $\tau_{3/2} = 1.1955(66)$ s. The residuals are shown in the bottom diagram.

which can be expressed in the form [9]

$$1/\tau_m = 1/\tau_{\text{nat}} + \sum_i \gamma_i, \tag{1}$$

where τ_m is the measured lifetime, τ_{nat} is the natural lifetime, and γ_i are the factors that contribute to the measured rate. All these factors are summarized in Table I.

The long-lifetime nature of the metastable $3d\ ^2D_{3/2}$ state of $^{40}Ca^+$ complicates the measurement owing to its high sensitivity to even rare collisions. Therefore, one of the main errors is introduced by collisions between the single ion and the background gases. These collisions quench the $3d\ ^2D_{3/2}$ state and result in a mixing of the two metastable states, $3d\ ^2D_{3/2}$ and $3d\ ^2D_{5/2}$ [9], thus reducing the measured lifetime. Usually, the collision probability is measured by monitoring the quantum jumps in the absence of the

TABLE I. Error evaluation for the measurement of the $3d\ ^2D_{3/2}$– state lifetime. The systematic errors consist of errors due to laser's intensities, collisions with background gases, and heating. The statistical error refers to the inherent error of data analysis.

Effect	Shift (ms)	Uncertainty (ms)
Fitting uncertainty		6.6
Collision and j mixing	0.5	0.3
Heating and ion loss		<0.1
397-nm laser power		<0.1
866-nm laser power		<0.1
397-nm shelving rate	−3.1	0.9
854-nm pumping rate	−1.7	0.6
Data analysis	4.1	4.1
Total error	−0.2	7.8

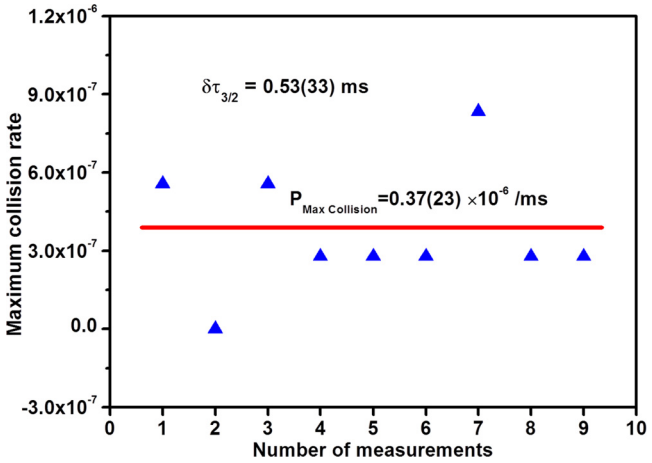

FIG. 5. The measured numbers of quantum jumps in the absence of the 729- and 854-nm lasers. The measurement is repeated nine times, and each period lasts 60 min. A maximum collision rate is $0.37(23) \times 10^{-6}$/ms, which contributes to the lifetime of the $3d\ ^2D_{3/2}$ state by $\delta\tau_{3/2} = 0.53(33)$ ms.

729- and 854-nm lasers. With a background pressure $<1.0 \times 10^{-8}$ Pa, an average of 0.022(14) quantum jump is observed every minute in different periods (12 quantum jumps are observed in 540 min), resulting in a maximum collision rate of $0.37(23) \times 10^{-6}$/ms. Hence, the lifetime of the $3d\ ^2D_{3/2}$ state is reduced by $\delta\tau_{3/2} = 0.53(33)$ ms. The measurement results are shown in Fig. 5.

Because the heating effect of the ion trap influences the measured lifetime, the rf-photon correlation method was adopted [30]. By precisely adjusting the voltages of the two dc field compensation electrodes and the two dc field endcap electrodes, the optimal parameter was selected, and the excess micromotion of the ion was minimized. The residual heating rate was measured by examining the time in which the fluorescence intensity returned to its original value after prolonged blocking of the cooling laser beam. No delay was observed when the blocking time was greater than 10 s. Since the longest wait time Δt was only 3 s in our experiment, this effect was negligible.

Furthermore, the laser power can also affect the measured lifetime. The impure spectra of the lasers induce undesirable excitations. The ac Stark effects caused by the lasers may couple with different atomic levels. In the experiment, two improvements were adopted to reduce the above factors. Because the spectrum of the 397-nm laser has a 393-nm component, which could induce a dipole transition from $4s\ ^2S_{1/2}$ to $4p\ ^2P_{3/2}$ during the detection period, a 406-nm narrowband optical filter was placed in the path of the 397-nm laser. The measured 397-nm transmittance reached 90%, while the 393-nm transmittance was below 0.46%. Because the power of the 397-nm laser was only $\sim$10.2 μW, the impurity component did not cause unnecessary excitation, and the influence of the 397-nm laser was thus negligible. During the wait time Δt, since the 729-nm laser was switched off by an AOM and the 854-nm laser was switched off by a mechanical shutter with a 60-dB extinction ratio, the influences of these two lasers were also negligible. Similarly, the 866-nm

laser spectrum could contain an 854-nm component, and thus, it could induce a dipole transition from $3d\ ^2D_{5/2}$ to $4p\ ^2P_{3/2}$ during the detection period. Therefore, two 866-nm narrowband optical filters were placed in the path of the 866-nm laser. As a result, the 866-nm laser transmittance reached 81%, and the 854-nm laser transmittance was below 0.027%. Consequently, this much weaker 854-nm impure component cannot induce the transition, and it can safely be ignored.

The shelving and pumping rates affect the measured lifetime. The 397-nm laser with 3 ms of time and 10.2 μW of power were used for incoherently shelving the ion to the $3d\ ^2D_{3/2}$ state without the 866-nm laser. The shelving rate was measured to be 0.9974(8) under these experimental conditions, which increased the measured lifetime and contributed to the lifetime of the $3d\ ^2D_{3/2}$ state by $\delta\tau_{3/2} = -3.1(9)$ ms. Similarly, if the 854-nm laser could not pump the ion from $3d\ ^2D_{5/2}$ to $4p\ ^2P_{3/2}$ when the second cycle started, the ion stayed in the former state for a while, which increased the measured lifetime. The 854-nm laser pumping rate was measured to be 0.9986(5) under the experimental conditions of 10 ms of time and 160 μW of power. The influence on the measured lifetime of the $3d\ ^2D_{3/2}$ state was $\delta\tau_{3/2} = -1.7(6)$ ms.

The other factors that may cause state detection errors were also analyzed in our experiment (see [11] for an evaluation of systematic errors). Poissonian noise in the PMT counts and the decay probability during the state detection period introduced a very small error. The probability ε_1 for incorrect state detection owing to the noise of the count rate depends on the discrimination between the $4s\ ^2S_{1/2}$ and $3d\ ^2D_{5/2}$ states performed by the electron-shelving technique. This is achieved by comparing the fluorescence count rates during the detection period with the application of a threshold value. In our experiment, during the 8-ms detection period, the average bright-state count was approximately 90, and the dark-state count was below 15. According to the threshold-setting equation [31], $\sigma = \sqrt{S_{\rm dark} \times S_{\rm bright}}$, where $S_{\rm dark}$ and $S_{\rm bright}$ are, respectively, the mean numbers of counts during the dark and fluorescing periods. We used a threshold value of 37. With this setting, the state detection error ε_1 was as small as 10^{-6} [31], which is much lower than the other errors. Consequently, this effect was neglected in our measurement. In addition, since the state detection requires the difference in fluorescence counts between the $4s\ ^2S_{1/2}$ and $3d\ ^2D_{5/2}$ states, the measurement requires a threshold to be set for screening. During the detection time, the ion will experience spontaneous emission, and thus, we introduce a probability ε_2 to take this detection error into account. The probability ε_2 was estimated by introducing the model function $1 - P = (1 - \varepsilon_2)\exp(-\Delta t/\tau_{3/2})$. A fitting to the experimental data described above yielded $\varepsilon_2 = 3.4(3.4) \times 10^{-3}$, which contributed to the lifetime of the $3d\ ^2D_{3/2}$ state by $\delta\tau_{3/2} = 4.1(4.1)$ ms. When the above factors were included in all the measured data points, they had no effect on the final result.

V. CONCLUSIONS

Combining the branching ratio in [32] with the measured lifetime of the metastable $3d\ ^2D_{3/2}$ state in this work, we can derive the $3d\ ^2D_{3/2} \rightarrow 4s\ ^2S_{1/2}$ transition matrix element (for the method, see [33]) $S_{ki} = 7.936(26)ea_0^2$, which agrees well with recent theoretical results [10,11,34]. Furthermore, by considering the lifetime of the $3d\ ^2D_{5/2}$ state that we measured in [10], the ratio between the lifetimes of $3d\ ^2D_{3/2}$ and $3d\ ^2D_{5/2}$ is determined to be 1.018(11), which is consistent with the previously calculated values of 1.0259(9) [11], 1.028 [14], 1.02 [17], 1.0175 [15], and 1.0335 [18].

In conclusion, we have precisely measured the lifetime of the $3d\ ^2D_{3/2}$ state by adopting a high-precision and highly synchronous measurement sequence for laser control and by recording the high-efficiency quantum jumps of a single $^{40}Ca^+$ ion confined in a miniature Paul trap. We have introduced an indirect method that allows us to correct the 729-nm pumping rate in a real-time way. The effective pumping rate can reach 100% even for different wait times. With this technique, all major errors have been mitigated to the level of 10^{-3}. Our final result for the measured lifetime of the $3d\ ^2D_{3/2}$ state is $\tau_{3/2} = 1.195(8)$ s. Our result is in agreement with the measured result of Barton *et al.* [9], as well as with the most recent theoretical values of Kreuter *et al.* [11] and Sahoo *et al.* [20]. Our result, however, disagrees with the measurement of Kreuter *et al.* [11]. Our method can be universally applied to lifetime measurements of other single ions and atoms with a similar structure. Nevertheless, since the largest errors in this measurement originate from the fitting uncertainty and collision effects, a further improvement in accuracy is possible by acquiring a larger number of quantum jumps under a better vacuum condition.

ACKNOWLEDGMENTS

We thank T. Shi, B. K. Sahoo, and C. Li for fruitful discussions. We thank Z. Yan for helpful comments on the manuscript. This work was financially supported by the National Basic Research Program of China (Grant No. 2012CB821301), by the National Natural Science Foundation of China (Grants No. 91336211, No. 11034009, No. 11474318, and No. 11304363), and by the Chinese Academy of Sciences.

[1] Y. Huang, H. Guan, P. Liu, W. Bian, L. Ma, K. Liang, T. Li, and K. Gao, Phys. Rev. Lett. **116**, 013001 (2016).

[2] F. Gebert, Y. Wan, F. Wolf, C. N. Angstmann, J. C. Berengut, and P. O. Schmidt, Phys. Rev. Lett. **115**, 053003 (2015).

[3] F. Schmidt-Kaler, H. Häffner, M. Riebe, S. Gulde, G. P. T. Lancaster, T. Deuschle, C. Becher, C. F. Roos, J. Eschner, and R. Blatt, Nature (London) **422**, 408 (2003).

[4] C. F. Roos, M. Chwalla, K. Kim, M. Riebe, and R. Blatt, Nature (London) **443**, 316 (2006).

[5] J. Benhelm, G. Kirchmair, C. F. Roos, and R. Blatt, Nat. Phys. **4**, 463 (2008).

[6] D. E. Welty, D. C. Morton, and L. M. Hobbs, Astrophys. J. Suppl. **106**, 533 (1996).

[7] J. Kwan and W. Fischer, Mon. Not. R. Astron. Soc. **411**, 2383 (2011).

[8] M. Hettrich, T. Ruster, H. Kaufmann, C. F. Roos, C. T. Schmiegelow, F. Schmidt-Kaler, and U. G. Poschinger, Phys. Rev. Lett. **115**, 143003 (2015).
[9] P. A. Barton, C. J. S. Donald, D. M. Lucas, D. A. Stevens, A. M. Steane, and D. N. Stacey, Phys. Rev. A **62**, 032503 (2000).
[10] H. Guan, H. Shao, Y. Qian, Y. Huang, P.-L. Liu, W. Bian, C.-B. Li, B. K. Sahoo, and K.-L. Gao, Phys. Rev. A **91**, 022511 (2015).
[11] A. Kreuter, C. Becher, G. P. T. Lancaster, A. B. Mundt, C. Russo, H. Häffner, C. Roos, W. Hänsel, F. Schmidt-Kaler, R. Blatt, and M. S. Safronova, Phys. Rev. A **71**, 032504 (2005).
[12] M. A. Ali and Y.-K. Kim, Phys. Rev. A **38**, 3992 (1988).
[13] C. J. Zeipen, Astron. Astrophys. **229**, 248 (1990).
[14] C. Guet and W. R. Johnson, Phys. Rev. A **44**, 1531 (1991).
[15] N. Vaeck, M. Godefroid, and C. Froese Fischer, Phys. Rev. A **46**, 3704 (1992).
[16] M. Poirier, Z. Phys. D **25**, 117 (1993).
[17] T. Brage, F. C. Froese, N. Vaeck, M. Godefroid, and A. Hibbert, Phys. Scr. **48**, 533 (1993).
[18] S. S. Liaw, Phys. Rev. A **51**, R1723 (1995).
[19] E. Biemont and C. J. Zeipen, Comments At. Mol. Phys. **33**, 29 (1996).
[20] B. K. Sahoo, Md. R. Islam, B. P. Das, R. K. Chaudhuri, and D. Mukherjee, Phys. Rev. A **74**, 062504 (2006).
[21] J. Jin and D. A. Church, Phys. Rev. Lett. **70**, 3213 (1993).
[22] M. Knoop, C. Champenois, G. Hagel, M. Houssin, C. Lisowski, M. Vedel, and F. Vedel, Eur. Phys. J. D **29**, 163 (2004).
[23] F. Arbes, F. Benzing, T. Gudjons, F. Kurth, and G. Werth, Z. Phys. D **29**, 159 (1994).
[24] M. Knoop, M. Vedel, and F. Vedel, Phys. Rev. A **52**, 3763 (1995).
[25] J. Lidberg, A. Al-Khalili, L.-O. Norlin, P. Royen, X. Tordoir, and S. Mannervik, J. Phys. B **32**, 757 (1999).
[26] N. Yu, W. Nagourney, and H. Dehmelt, Phys. Rev. Lett. **78**, 4898 (1997).
[27] M. Ramm, T. Pruttivarasin, M. Kokish, I. Talukdar, and H. Häffner, Phys. Rev. Lett. **111**, 023004 (2013).
[28] W. Bian, Y. Huang, H. Guan, P. Liu, L. Ma, and K. Gao, Rev. Sci. Instrum **87**, 063121 (2016).
[29] W. Qu, Y. Huang, H. Guan, X. Huang, and K. Gao, Chin. J. Lasers **38**, 0802008 (2011).
[30] D. J. Berkeland, J. D. Miller, J. C. Bergquist, W. M. Itano, and D. J. Wineland, J. Appl. Phys. **83**, 5025 (1998).
[31] C. Roos, Ph.D. thesis, University of Innsbruck, 2000.
[32] C. Auchter, T. W. Noel, M. R. Hoffman, S. R. Williams, and B. B. Blinov, Phys. Rev. A **90**, 060501(R) (2014).
[33] D. K. Nandy, Y. Singh, B. K. Sahoo, and C. Li, J. Phys. B **44**, 225701 (2011).
[34] U. I. Safronova and M. S. Safronova, Can. J. Phys. **89**, 465 (2011).